Advances in Pharmacological and Pharmaceutical Sciences

WILEY

RESEARCH ARTICLE OPEN ACCESS

Salvianolic Acid Activates ATP-Driven Mitochondrial Biogenesis to Suppress the Epithelial–Mesenchymal Transition in LNCaP Prostate Cancer Cells

Hsing-Chia Mai[1,2,3] | Pei-Fang Hsieh[4,5] | Chun-Hsien Wu[1,3,4,6] | Richard C. Wu[2,4,6] | Sih-Han Chen[2,4,6] | Wei-Lun Huang[2,3,4] | Yu-Lin Yang[5,7] | Victor C. Lin[3,4] | Chiang-Ting Wang[8,9]

[1]Department of Urology, E-Da Cancer Hospital, Kaohsiung, Taiwan | [2]Department of Nursing, I-Shou University, Kaohsiung, Taiwan | [3]School of Medicine, College of Medicine, I-Shou University, Kaohsiung, Taiwan | [4]Division of Urology, Department of Surgery, E-Da Hospital, Kaohsiung, Taiwan | [5]Department of Medical Laboratory Science and Biotechnology, Chung-Hwa University of Medical Technology, Tainan, Taiwan | [6]Department of Information Engineering, I-Shou University, Kaohsiung, Taiwan | [7]Graduate Institute of Biomedical Science, Chung-Hwa University of Medical Technology, Tainan, Taiwan | [8]Division of Urology, Department of Surgery, Kaohsiung Armed Forces General Hospital, Kaohsiung, Taiwan | [9]Division of Urology, Gangshan Branch, Kaohsiung Armed Forces General Hospital, Kaohsiung, Taiwan

Correspondence: Victor C. Lin (victorlin0098@gmail.com) | Chiang-Ting Wang (wct5816@gmail.com)

Received: 5 April 2025 | **Revised:** 17 December 2025 | **Accepted:** 26 December 2025

Academic Editor: Mounir Tilaoui

Keywords: epithelial–mesenchymal transition | LNCaP cells | mitochondrial biogenesis | prostate cancer | salvianolic acid

ABSTRACT

Background: Prostate cancer is among the most frequently identified malignant tumors in men. Epithelial–mesenchymal transition (EMT) serves as a key process driving tumor development and enabling cancer cells to spread to remote tissues. Salvianolic acid (SA), a polyphenolic compound derived from *Salvia miltiorrhiza*, exhibits potential anticancer effects. This research explores the impact of SA on the regulation of EMT and mitochondrial biogenesis in LNCaP and LNCaP-Enz-R prostate cancer cells.

Methods: The effects of SA on cell viability, migration, and mitochondrial function were assessed using MTT assay, wound healing assay, and JC-1 staining. Western blotting was conducted to assess the levels of EMT-related markers (E-cadherin, Snail, α-SMA, and Slug) along with critical regulators of mitochondrial biogenesis, such as AMP-activated protein kinase (AMPK), PGC-1α, SIRT1, and NRF1. ATP production and mitochondrial membrane potential ($\Delta\Psi$m) were measured to evaluate mitochondrial activity.

Results: SA significantly inhibited the expansion, viability, and movement of LNCaP and LNCaP-Enz-R cells. SA administration significantly inhibited EMT, as indicated by increased E-cadherin expression and reduced expression of α-SMA, Snail, and Slug. Moreover, SA promoted mitochondrial biogenesis by activating the AMPK/PGC-1α/SIRT1/NRF1 pathway, resulting in enhanced ATP generation and maintenance of $\Delta\Psi$m.

Conclusion: SA exhibited strong anticancer effects in prostate cancer cells by inhibiting EMT and stimulating mitochondrial biogenesis, further interfering with tumor progression. Reportedly, SA can be a promising treatment option for prostate cancer.

Hsing-Chia Mai and Pei-Fang Hsieh made equal contributions to this study.

This is an open access article under the terms of the Creative Commons Attribution License, which permits use, distribution and reproduction in any medium, provided the original work is properly cited.

Copyright © 2026 Hsing-Chia Mai et al. *Advances in Pharmacological and Pharmaceutical Sciences* published by John Wiley & Sons Ltd.

1 | Introduction

Prostate cancer is the second most frequently detected malignancy and continues to be a major contributor to cancer-related deaths among men globally [1]. Despite advancements in diagnosis and treatment, many patients eventually develop advanced-stage disease, particularly castration-resistant prostate cancer (CRPC) [2–4], which often has a poor prognosis and limited therapeutic options [5, 6]. Epithelial–mesenchymal transition (EMT) is a key molecular mechanism driving prostate cancer progression and therapeutic resistance [7]. This biological process enhances cancer cell plasticity, facilitating migration, invasion, and metastasis [4, 8]. EMT involves the downregulation of epithelial markers such as E-cadherin, along with the increased expression of mesenchymal markers like smooth muscle actin (SMA), Snail, and Slug [9]. Because EMT is strongly linked to metastasis and treatment resistance, it has become a primary focus in the development of novel anticancer therapies [10].

Apart from EMT, metabolic reprogramming and mitochondrial dysfunction are crucial hallmarks of cancer that adapt tumor cells for the high energy demands required for uncontrolled growth and metastasis [11–13]. As the primary sites of ATP production and regulators of cellular metabolism, mitochondria are crucial in cancer cell survival [12]. Prostate cancer cells, in particular, rely on mitochondrial biogenesis and metabolic plasticity to promote their growth and overcome therapeutic challenges. The AMP-activated protein kinase (AMPK) pathway is essential for regulating mitochondrial biogenesis and preserving cellular energy homeostasis, emphasizing its viability as a therapeutic target for multiple diseases [14–22]. This pathway is often dysregulated in cancer cells and contributes to their enhanced proliferative and migratory capacity. Thus, strategies aimed at restoring mitochondrial function and regulating the AMPK/SIRT1/PGC-1α pathway may provide therapeutic advantages for prostate cancer treatment.

Salvianolic acid (SA), a polyphenol extracted from *Salvia miltiorrhiza*, exhibits diverse pharmacological effects, such as antioxidant, anti-inflammatory, and anticancer activities [14–27]. SA exhibits antitumor activity across various cancers by modulating critical signaling pathways that govern cell survival, apoptosis, and metastasis. However, the specific effects of SA on EMT and mitochondrial biogenesis in prostate cancer cells remain largely unexplored.

Recognizing the pivotal involvement of EMT and mitochondrial function in prostate cancer progression, this study explores the molecular mechanisms through which SA exerts its anticancer effects in LNCaP and LNCaP-Enz-R prostate cancer cells. Specifically, we hypothesized that SA suppresses cancer cell viability, migration, and EMT by modulating mitochondrial biogenesis-related signaling pathways, including AMPK, SIRT1, PGC-1α, and nuclear respiratory factor 1 (NRF1). To test this hypothesis, we analyzed the impact of SA on EMT marker expression, mitochondrial biogenesis, ATP generation, and mitochondrial membrane potential ($\Delta\Psi$m). Our integrated findings would provide novel insights into the therapeutic potential of SA and its dual role in targeting EMT and mitochondrial function in prostate cancer.

This research aims to explore the molecular mechanisms of SA and assess its viability as a treatment approach for prostate cancer, with an emphasis on CRPC.

2 | Materials and Methods

2.1 | Cell Culture

LNCaP cells were obtained from the American Type Culture Collection (Rockville, MD, USA) and cultured in Dulbecco's Modified Eagle Medium (Thermo Fisher Scientific, Waltham, MA, USA) with the addition of 10% fetal bovine serum (Thermo Fisher Scientific). Cultivation was carried out at 37°C in a humidified chamber under a 5% CO_2 environment. Enzalutamide-resistant LNCaP cell lines (LNCaP-Enz-R) were generated by continuous exposure of LNCaP cells to enzalutamide (5 μM) for over 6 months. The LNCaP-Enz-R cells used in this study were kindly provided by Dr. See-Tong Pang.

2.2 | Reagent

SA B (B7186, Sigma-Aldrich, MO, USA) was initially dissolved in DMSO to create a high-concentration stock solution. Before application, the stock solution was mixed with the culture medium to achieve the required working concentrations. To avoid possible cytotoxicity, the final DMSO content in the culture medium was maintained at $< 0.1\%$. Cells were treated with AICAR (1 mM; Sigma-Aldrich, A9978) [14] or Compound C (10 μM; Sigma-Aldrich, P5499) [15] for 24 h as AMPK activator and inhibitor, respectively.

2.3 | Cell Viability Assay

LNCaP and LNCaP-Enz-R cells were seeded at a density of 5×10^3 cells per well in 96-well plates and incubated overnight for attachment prior to treatment with varying concentrations of SA (0–400 μM). The MTT assay was performed to assess cell viability. LNCaP and LNCaP-Enz-R cells were seeded into 96-well plates at a predetermined density and treated with varying concentrations of SA B (0–400 μM). Following incubation, 20 μL of MTT reagent (5 mg/mL in PBS) was added to each well, and the plates were incubated at 37°C for an additional 4 h. The resulting formazan crystals were dissolved in 100 μL of DMSO, and absorbance was recorded at 570 nm using a microplate reader. Cell growth was evaluated relative to the untreated control group [28].

2.4 | Cell Migration Assay

For the migration assay, 3×10^5 cells per well were plated in 6-well plates and allowed to reach approximately 90% confluence before the culture insert was removed to create a wound gap. Cells were then treated with SA under serum-free conditions for 24 h. Cell motility was evaluated using Ibidi Culture-Inserts (Ibidi, Gräfelfing, Germany). LNCaP and LNCaP-Enz-R cells were seeded into 6-well plates, with a culture insert placed at the center of each well. Once the cells attained approximately 90% confluence, the inserts were gently removed, creating a cell-free gap. The cells were exposed to different doses of SA B in a serum-free environment and maintained in incubation for 24 h. The movement of cells into the created gap was monitored between 0 and 24 h after treatment with an Olympus DP71 light microscope (Olympus, Tokyo, Japan). Microscopic images were captured at various time points, and the extent of cell migration was analyzed using ImageJ. The wound closure rate was calculated by comparing the initial and final gap dimensions in relation to the

original area. Each experiment was conducted three times to confirm reproducibility [29].

2.5 | Western Blot Analysis

Cells were seeded at 5×10^5 cells per well in 6-well plates and cultured until ~80% confluence before treatment. After incubation with SA for 24 h, cells were lysed for total protein extraction. The cells were lysed in RIPA buffer (Thermo Fisher Scientific) containing 1 × protease and phosphatase inhibitors (Thermo Fisher Scientific) and incubated on ice for 30 min to ensure complete protein isolation. The lysates were spun at $12{,}000 \times g$ for 15 min at 4°C, and the supernatant was meticulously collected. Protein amounts were later assessed using a BCA protein assay kit (Thermo Fisher Scientific).

Each 30 μg protein sample was resolved on 10% SDS–PAGE gels and then transferred onto PVDF membranes (MilliporeSigma, Burlington, MA, USA) using the wet transfer method. To block nonspecific binding, the membranes were incubated in 5% skim milk diluted in TBST for 1 h at room temperature. Subsequently, they were stored overnight at 4°C with primary antibodies targeting specific proteins. EMT markers: E-cadherin (ab53033, 1:2000; Abcam, Cambridge, UK), α-SMA (ab5694, 1:2000; Abcam), Snail (ab216347, 1:2000; Abcam), Slug (ab302780, 1:2000; Abcam) Mitochondrial biogenesis-related proteins: AMPK (ab32047, 1:2000; Abcam), SIRT1 (ab110304, 1:2000; Abcam), PGC-1α (ab54481, 1:2000; Abcam), NRF1 (ab34682, 1:2000; Abcam), and β-actin (A5441, 1:4000; Sigma-Aldrich, St. Louis, MO, USA)

After being rinsed three times with TBST, the membranes were exposed to HRP-conjugated secondary antibodies (1:5000 dilution) and kept at ambient temperature for 1 h. Protein bands were detected using the Western-Ready ECL Substrate Plus Kit (426,316, BioLegend, San Diego, CA, USA) and captured with the MultiGel-21 imaging system (Bio-Rad Laboratories, Hercules, CA, USA). Band intensity was analyzed using ImageJ software, with β-actin used as a reference for normalization [30].

2.6 | JC-1 Staining for Detecting the ΔΨm

The JC-1 Mitochondrial Membrane Potential Assay Kit (Cayman Chemical, Ann Arbor, MI, USA) was utilized to evaluate $\Delta\Psi$m per the manufacturer's instructions. LNCaP and LNCaP-Enz-R cells were seeded at 2×10^5 cells per well in 6-well plates and treated with SA for 24 h before JC-1 staining was performed to assess the $\Delta\Psi$m. This kit provides all necessary reagents and detailed protocols for analyzing mitochondrial integrity in whole cells. LNCaP and LNCaP-Enz-R cells were grown in six-well plates and exposed to different doses of SA B for a full day. Once incubation was completed, the cells were collected, rinsed two times with PBS, and resuspended in 500 μL of JC-1 staining mixture, which was created by combining the JC-1 dye reagent with assay buffer at a 1:9 ratio. The cell mixture was subsequently kept at 37°C for 30 min in darkness, enabling the dye to accumulate within the mitochondria. After incubation, the cells were washed two times with PBS to remove residual dye and immediately analyzed using a fluorescence plate reader. For JC-1 monomers, the excitation/emission wavelengths are approximately 510/527 nm, whereas for JC-1 aggregates, they are approximately 585/590 nm. $\Delta\Psi$m was evaluated by quantifying the red-to-green fluorescence ratio, in which a decrease in value indicates mitochondrial depolarization. To enhance data reliability and precision, all experiments were conducted in triplicate [31].

2.7 | Statistical Analysis

All experiments were independently performed in triplicate, and the results were presented as mean ± standard deviation (SD). Statistical analysis was conducted using one-way ANOVA, followed by Tukey's post hoc test for multiple comparisons. ANOVA determined the overall variations among groups, while Tukey's method identified significant differences between specific pairs, reducing the risk of family-wise error in multiple comparisons. $p > 0.05$ was considered statistically significant. All data analyses were conducted utilizing GraphPad Prism (Version 9).

3 | Results

3.1 | SA Dose-Dependently Reduced the Viability and Activity of Hormone-Sensitive and -Resistant Prostate Cancer Cells

The IC_{50} of SA was not determined in this study, as the purpose of the assay was to evaluate the relative changes in cell viability across different concentrations rather than to assess cytotoxic potency [24, 32]. The effect of different SA doses (0–400 μM) on tumor cell growth and survival was examined in hormone-dependent LNCaP cells and hormone-independent LNCaP-Enz-R cells. Treatment with SA in LNCaP cells resulted in a dose-dependent reduction in cell viability, indicating its potential to suppress cancer cell growth in hormone-responsive prostate cancer (Figure 1(a)). Similarly, LNCaP-Enz-R cells exposed to SA exhibited a similar dose-dependent reduction in viability, emphasizing its suppressive impact on hormone-resistant prostate cancer cells (Figure 1(b)). These results emphasize the potent inhibitory effect of SA on prostate cancer cell viability and survival, demonstrating similar effectiveness across hormone-responsive and hormone-resistant types.

3.2 | SA Inhibited EMT and Migration in LNCaP and LNCaP-Enz-R Cells by SA Treatment

The effect of SA on EMT markers in LNCaP and LNCaP-Enz-R cells was evaluated by analyzing key proteins associated with the epithelial and mesenchymal phenotypes. A 24-h incubation period was chosen to evaluate the early effects of SA on migration and EMT-related signaling before significant cell proliferation occurs, given that the doubling time of LNCaP cells is approximately 48–60 h. As shown in Figure 2(a), increasing SA concentrations (0–400 μM) led to a dose-dependent upregulation of the epithelial marker E-cadherin, while simultaneously decreasing the mesenchymal marker α-SMA expression in LNCaP cells. Moreover, the levels of EMT-associated transcription factors Snail and Slug were significantly reduced in a concentration-dependent manner. Western blot quantification further validated the impact of SA on EMT-related protein regulation in LNCaP cells (Figure 2(b)). Wound healing assays revealed that SA exposure gradually suppressed the migration capacity of LNCaP cells in a concentration-dependent manner

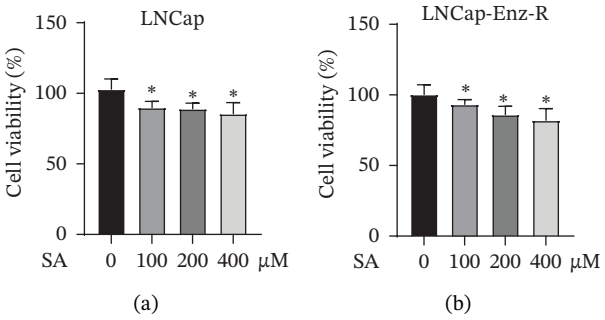


FIGURE 1 | Salvianolic acid (SA) dose-dependently reduced the cell viability and activity of hormone-sensitive and -resistant prostate cancer cells. (a) SA treatment dose-dependently reduced the viability of LNCaP cells, indicating the suppression of cancer cell activity. (b) Similarly, LNCaP-Enz-R cells treated with SA showed significantly decreased viability in a dose-dependent manner, further promoting the inhibitory effect of SA on prostate cancer cell activity across different phenotypes. Data are expressed as the mean ± standard deviation of three independent experiments. Statistical significance was determined using one-way analysis of variance followed by Tukey's post hoc test ($^{*}p < 0.05$).

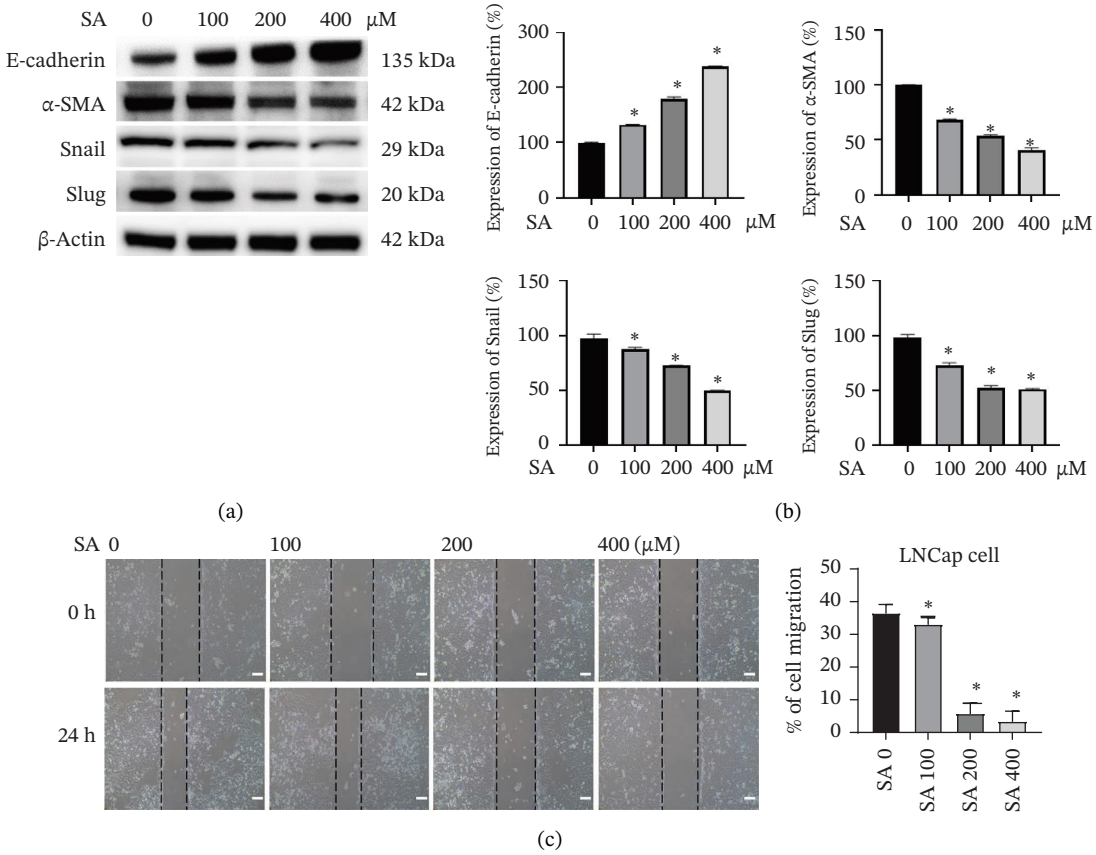


FIGURE 2 | (Continued)

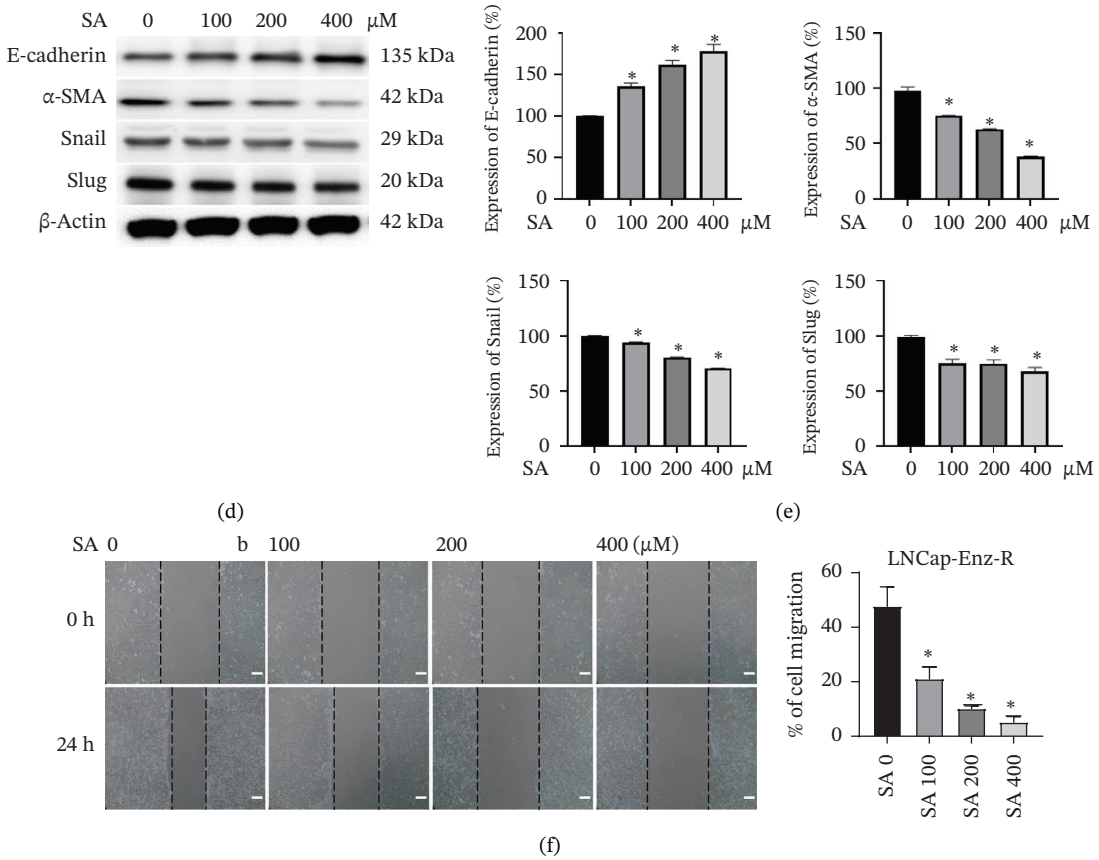


FIGURE 2 | Effect of salvianolic acid (SA) on epithelial–mesenchymal transition (EMT) and cell migration in LNCaP and LNCaP-Enz-R cells. (a) Western blot analysis showed that treatment of LNCaP cells with increasing SA concentrations (0–400 μM) dose-dependently upregulated the epithelial marker E-cadherin and downregulated the mesenchymal marker α-SMA. EMT-associated transcription factors Snail and Slug were also significantly and dose-dependently reduced. (b) Quantification of protein expression in panel (a) confirmed the dose-dependent effects of SA on EMT-related markers in LNCaP cells. (c) Migration assays revealed that SA treatment significantly and dose-dependently suppressed the migratory ability of LNCaP cells. Representative wound-healing images at 0 and 24 h. Scale bar = 50 μm. (d) In LNCaP-Enz-R cells, SA treatment similarly increased the expression of E-cadherin, decreased α-SMA levels, and dose-dependently downregulated snail and slug. (e) Quantitative analysis of protein expression in panel (d) confirmed the inhibitory effects of SA on EMT-related markers in LNCaP-Enz-R cells. (f) Migration assays demonstrating that SA treatment effectively impaired the migratory capacity of LNCaP-Enz-R cells in a dose-dependent manner. The quantitative results are now provided in Figures 2(c) and 2(f) and show a significant, dose-dependent inhibition of wound closure by salvianolic acid in LNCaP-Enz-R cells (exact p values indicated in the figure). Data are expressed as the mean ± standard deviation of three independent experiments. Statistical significance was determined using one-way analysis of variance with Tukey's post hoc test ($^*p < 0.05$).

(Figure 2(c)). Higher SA concentrations showed more effectively inhibited cancer cell movement than untreated controls (Figure 2(d)). Similarly, SA treatment of LNCaP-Enz-R cells increased E-cadherin expression, decreased α-SMA levels, and downregulated Snail and Slug in a dose-dependent fashion, indicating that SA also suppressed EMT in this cell line. Quantitative analysis of the western blot results confirmed the inhibitory effects of SA on EMT-related markers in LNCaP-Enz-R cells (Figure 2(e)). Migration assays also demonstrated that SA treatment significantly and dose-dependently impaired the migratory ability of LNCaP-Enz-R cells, confirming the role of SA in suppressing the metastatic potential of prostate cancer cells (Figure 2(f)).

Therefore, SA successfully suppressed EMT and cell motility in LNCaP and LNCaP-Enz-R cells by regulating essential epithelial and mesenchymal markers along with their associated transcriptional regulators.

3.3 | SA Activated Mitochondrial Biogenesis-Associated Proteins in LNCaP and LNCaP-Enz-R Cells

Treatment with SA significantly upregulated proteins associated with mitochondrial biogenesis in LNCaP and LNCaP-Enz-R prostate cancer cells. Western blot analysis demonstrated that SA treatment induced a concentration-dependent upregulation of AMPK, SIRT1, PGC1, NRF1, and TFAM expression in LNCaP cells (Figure 3(a)). Quantitative analysis confirmed the dose-dependent upregulation of these mitochondrial biogenesis-related proteins in LNCaP cells (Figure 3(b)). Similarly, treatment with SA in LNCaP-Enz-R cells dose-dependently increased the expression of AMPK, SIRT1, PGC1, NRF1, and TFAM on Western blot analysis (Figure 3(c)). Quantitative analysis of protein expression in LNCaP-Enz-R cells further corroborated the dose-dependent effects of SA on mitochondrial biogenesis (Figure 3(d)).

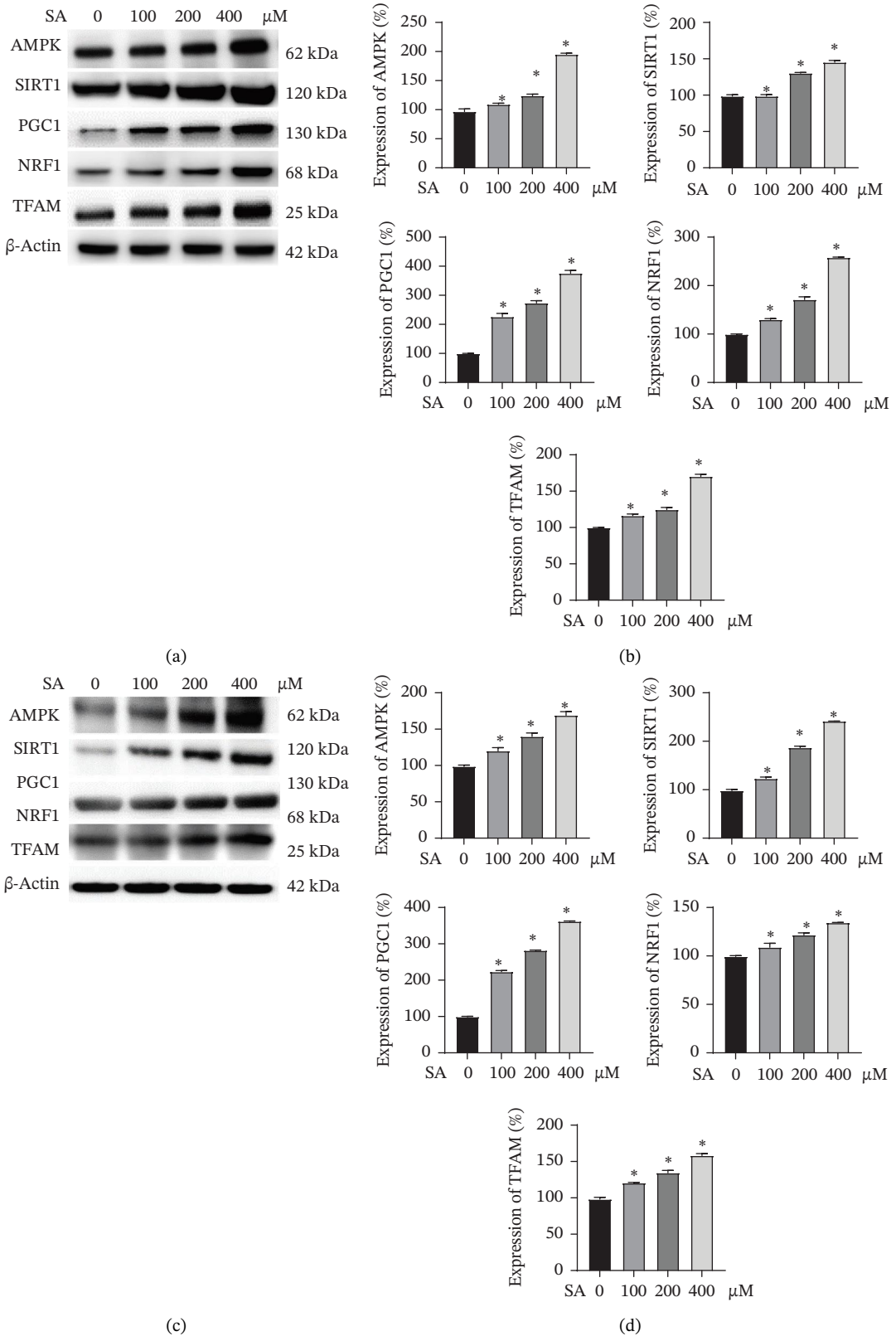


FIGURE 3 | Effect of salvianolic acid (SA) on mitochondrial biogenesis-associated proteins in LNCaP and LNCaP-Enz-R cells. (a) Western blot analysis of LNCaP cells treated with SA (0–400 μM) showed a dose-dependent increase in the expression of mitochondrial biogenesis-related proteins AMPK, SIRT1, PGC1, NRF1, and TFAM. (b) Quantitative analysis of protein expression levels in (a) demonstrating the significant upregulation of these markers in LNCaP cells with SA treatment. (c) Similarly, treatment of LNCaP-Enz-R cells with SA dose-dependently upregulated AMPK, SIRT1, PGC1, NRF1, and TFAM levels. (d) Quantitative analysis of (c) further confirmed the dose-dependent effects of SA on the upregulation of mitochondrial biogenesis-associated proteins in LNCaP-Enz-R cells. Data are expressed as the mean ± standard deviation of three independent experiments. Statistical significance was determined using one-way analysis of variance with Tukey's post hoc test ($^{*}p < 0.05$).

These findings demonstrate that SA enhanced mitochondrial biogenesis by dose-dependently upregulating key regulatory proteins in LNCaP and LNCaP-Enz-R prostate cancer cells.

3.4 | SA Regulated EMT-Related Proteins via the AMPK Signaling Pathway in LNCaP and LNCaP-Enz-R Cells

To determine whether SA influences EMT through AMPK signaling, LNCaP and LNCaP-Enz-R cells were treated with SA (400 μM) alone or in combination with AICAR, an AMPK activator, or Compound C, an AMPK inhibitor. SA treatment markedly increased E-cadherin expression while decreasing the levels of α-SMA, Snail, and Slug in LNCaP cells. AICAR produced a comparable effect by further enhancing E-cadherin expression and downregulating α-SMA, Snail, and Slug. In contrast, co-administration with Compound C counteracted these effects, preventing SA-induced upregulation of E-cadherin and downregulation of α-SMA, Snail, and Slug (Figure 4(a)). The quantification of these alterations is depicted in Figure 4(b). A comparable pattern was observed in LNCaP-Enz-R cells, where SA treatment enhanced E-cadherin expression while decreasing the levels of α-SMA, Snail, and Slug. These effects were amplified by AICAR but reversed by Compound C (Figure 4(c)). The quantitative results of these findings are shown in Figure 4(d).

These results demonstrate that SA modulated EMT-related protein expression in LNCaP and LNCaP-Enz-R cells through the AMPK signaling pathway.

3.5 | Effects of SA on ATP Production and ΔΨm in LNCaP and LNCaP-Enz-R Cells

ATP levels and $\Delta\Psi$m were analyzed using JC-1 staining to verify whether SA stimulation of LNCaP cells enhances mitochondrial biogenesis and regulates ATP production. An ATP standard curve was generated to quantify ATP production in the experimental setup (Figure 5(a)). Stimulation of LNCaP cells with SA significantly increased ATP levels in a dose-dependent manner, indicating enhanced mitochondrial activity (Figure 5(b)). Similarly, SA stimulation of LNCaP-Enz-R cells caused a dose-dependent increase in ATP levels, further confirming its role in mitochondrial energy production (Figure 5(c)).

JC-1 staining was utilized to assess alterations in $\Delta\Psi$m. In functional mitochondria with elevated $\Delta\Psi$m, JC-1 dye aggregates, producing red fluorescence (J-aggregates), whereas in compromised or depolarized mitochondria with diminished $\Delta\Psi$m, the dye remains in its monomeric state, emitting green fluorescence. The red-to-green fluorescence ratio serves as an indicator of mitochondrial integrity. LNCaP cells treated with SA exhibited a concentration-dependent rise in red fluorescence, signifying J-aggregate formation, coupled with a decline in green fluorescence, suggesting stabilization and enhancement of $\Delta\Psi$m (Figure 5(d)). Similarly, SA treatment of LNCaP-Enz-R cells dose-dependently increased red fluorescence and decreased green fluorescence, demonstrating improved mitochondrial function and reduced depolarization (Figure 5(e)).

These findings demonstrate that SA enhanced mitochondrial biogenesis and improved mitochondrial function, as evidenced by an increase in ATP production and the stabilization of the $\Delta\Psi$m.

4 | Discussion

We investigated the impact of SA on EMT and cellular migration in LNCaP and enzalutamide-resistant LNCaP (LNCaP-Enz-R) cells. SA significantly downregulated critical EMT and mesenchymal markers, including E-cadherin, α-SMA, Snail, and Slug, while also reducing cell motility. Additionally, SA exerted these effects by stimulating mitochondrial biogenesis pathways and enhancing $\Delta\Psi$m, highlighting mitochondrial health as a crucial factor in EMT regulation within prostate cancer cells.

A major discovery of this research is the upregulation of proteins associated with mitochondrial biogenesis, including AMPK, SIRT1, PGC-1α, and NRF1. These proteins are crucial in the regulation of mitochondrial function and energy metabolism. AMPK, a key regulator of cellular energy, promotes mitochondrial biogenesis by activating PGC-1α, which in turn regulates the genes involved in mitochondrial DNA replication and the synthesis of mitochondrial proteins. Our findings that SA activates AMPK and upregulates PGC-1α suggest that SA may enhance mitochondrial function by increasing the mitochondrial mass and activity. Activating the AMPK–PGC-1α axis improves cellular energy homeostasis, a critical process in cell survival and function, particularly under stressful conditions, such as those encountered during cancer progression. Similarly, SIRT1, an NAD^+-dependent deacetylase, is essential in mitochondrial biogenesis and oxidative stress resistance. SIRT1 can enhance mitochondrial function and protect against cellular damage by deacetylating various target proteins involved in metabolism, inflammation, and cell survival. Within cancer progression, SIRT1 plays a role in modulating EMT by inhibiting metastasis-associated pathways while enhancing epithelial traits [14, 33]. The upregulation of these key mitochondrial regulators in response to SA treatment indicates that SA could promote mitochondrial health, enhance cellular energy production, and suppress EMT.

The increase in $\Delta\Psi$m, as measured by the JC-1 assay, further confirms that SA promotes mitochondrial integrity and function. $\Delta\Psi$m serves as an essential marker of mitochondrial function. A reduction in membrane potential signifies mitochondrial dysfunction and is often associated with the onset of apoptosis. A significant enhancement in $\Delta\Psi$m indicates that SA could improve mitochondrial function, thereby potentially boosting cellular ATP production and creating a favorable, energy-rich environment for epithelial cell characteristics. This result aligns with previous studies indicating that preserving mitochondrial activity limits cancer cell movement and spread by suppressing EMT. Moreover, maintaining mitochondrial integrity can lower reactive oxygen species production, which could otherwise trigger cellular stress and promote cancer cell invasiveness [15, 34–36].

Furthermore, apart from its influence on mitochondrial activity, SA treatment was observed to increase E-cadherin expression while reducing the levels of α-SMA, Snail, and Slug, all of which are widely recognized as key indicators of EMT. Snail and Slug function as transcriptional regulators that suppress E-cadherin, a crucial adhesion protein, while enhancing mesenchymal marker expression like α-SMA. Elevated E-cadherin levels contribute to stronger cell–cell adhesion, which is essential for preserving the epithelial state and limiting cellular motility. Conversely, Snail and Slug promote a mesenchymal phenotype,

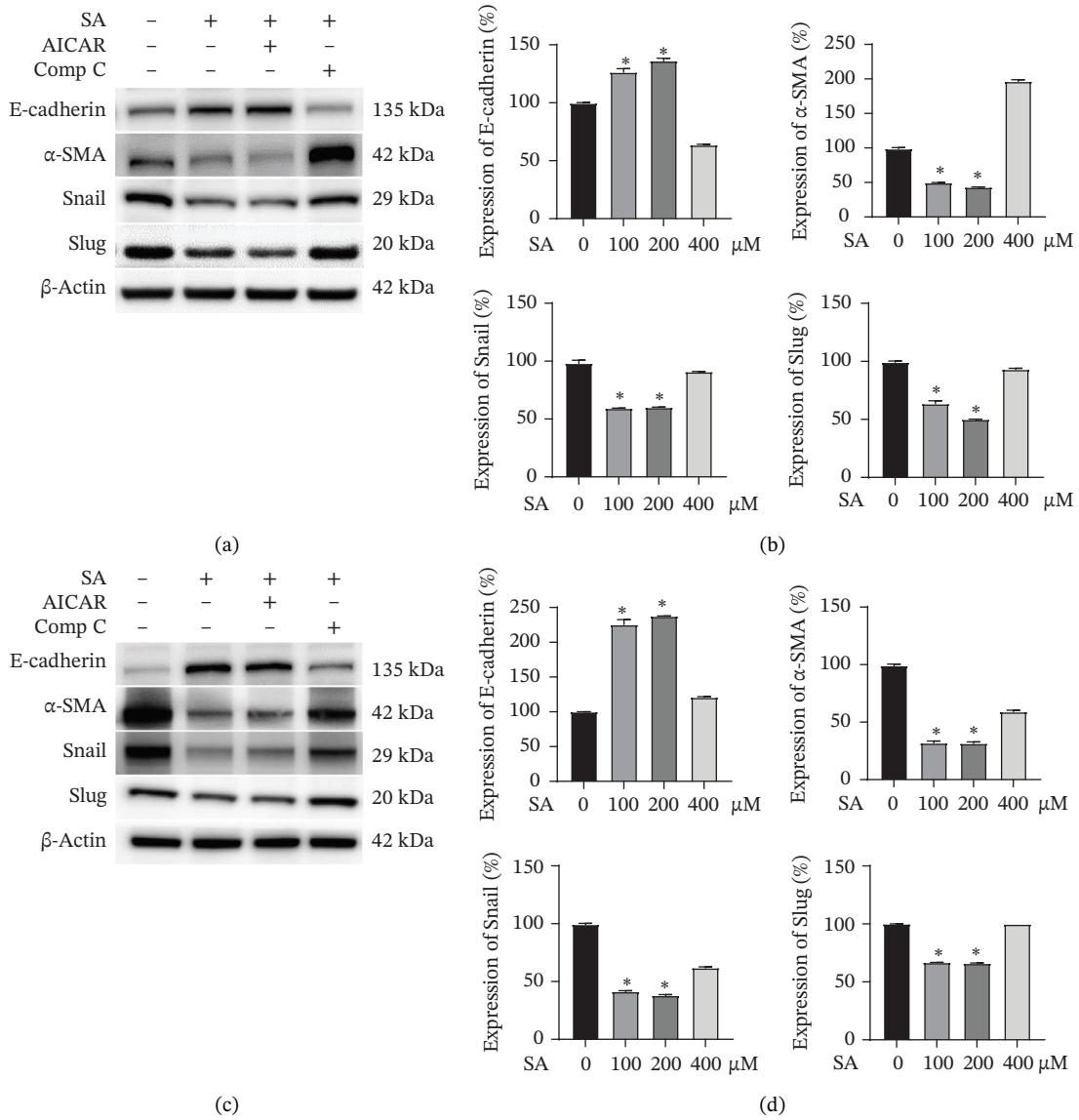


FIGURE 4 | Salvianolic acid (SA) modulates EMT-related protein expression through AMPK signaling in LNCaP and LNCaP-Enz-R cells. (a) In LNCaP cells, treatment with SA (400 μM) increased E-cadherin expression and decreased that of α-SMA, Snail, and Slug. The addition of AICAR (AMPK activator) enhanced these effects, whereas Compound C (AMPK inhibitor) reversed them, inhibiting the regulatory effect of SA on EMT markers. (b) Quantification of the protein expression changes observed in (a). (c) In LNCaP-Enz-R cells, SA treatment similarly increased E-cadherin expression and reduced that of α-SMA, Snail, and Slug. Cotreatment with AICAR enhanced these changes, whereas compound C abrogated the effects of SA on EMT markers. (d) Quantification of the protein expression changes observed in (c). Data are expressed as the mean ± standard deviation of three independent experiments. Statistical significance was determined by one-way analysis of variance followed by Tukey's post hoc test ($^*p < 0.05$).

which enhances the invasive potential of cancer cells [15, 25–27]. The ability of SA to reverse these EMT-associated changes indicates that it may disrupt the pathways responsible for inducing cell motility and metastasis. This is particularly relevant in the context of enzalutamide-resistant prostate cancer, where EMT is a key contributor to treatment failure and disease progression [3, 37–39]. Thus, the inhibition of EMT by SA could provide a novel strategy for overcoming resistance to androgen deprivation therapies, such as enzalutamide, which are standard treatments for advanced prostate cancer.

Furthermore, the suppression of cell migration observed in this study, as demonstrated by the wound healing assays, further confirms that SA can inhibit the metastatic potential of prostate cancer cells. The ability of SA to inhibit cell migration is likely linked to its effects on mitochondrial biogenesis and on the regulation of EMT markers. Cancer cell migration is highly energy-dependent; thus, cells with dysfunctional mitochondria are often less capable of sustaining the energy demands required for motility [11, 13, 18, 40–43]. The ability of SA to enhance mitochondrial function and suppress EMT contributes to its ability to reduce cell migration among prostate cancer cells, thereby decreasing their metastatic potential.

This research has certain limitations. First, the impact of SA was assessed solely in LNCaP and LNCaP-Enz-R prostate cancer cell lines, which may not completely represent the diverse heterogeneity of prostate cancer. Another limitation of this study is that normal prostate epithelial cells were not included as a control. Because the main objective was to compare the differential

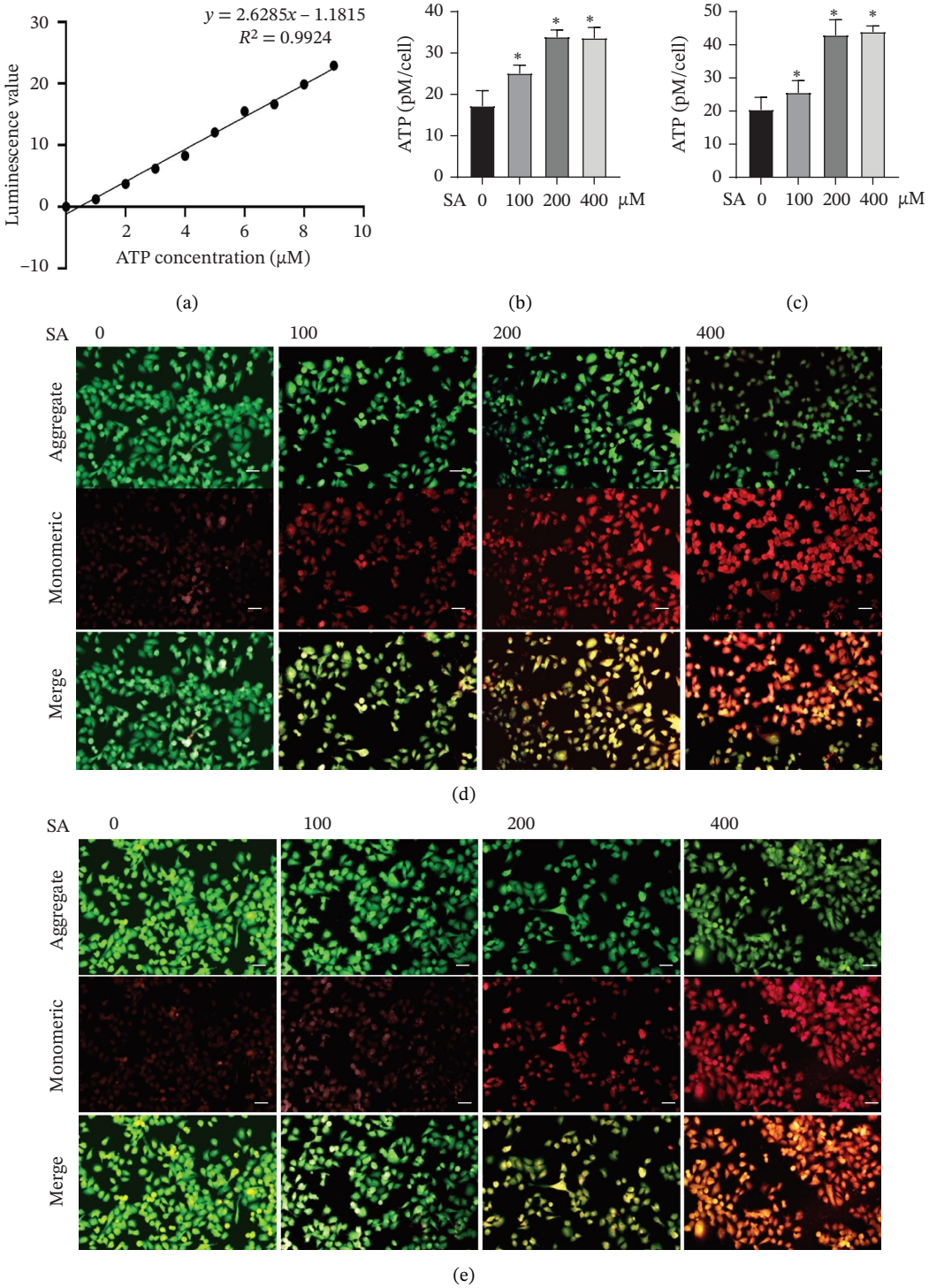


FIGURE 5 | Effect of salvianolic acid (SA) on ATP production and mitochondrial membrane potential in LNCaP and LNCaP-Enz-R cells. (a) A standard curve was generated using ATP standards to quantify the ATP levels in the experimental setup. (b) Treatment with SA dose-dependently increased ATP production in LNCaP cells, demonstrating enhanced mitochondrial energy output. (c) Similarly, SA treatment dose-dependently increased ATP levels in LNCaP-Enz-R cells. (d) JC-1 staining revealed that SA treatment of LNCaP cells increased red fluorescence (J-aggregates, indicating polarized mitochondria) and decreased green fluorescence (monomers, indicating depolarized mitochondria), indicating enhanced mitochondrial membrane potential. (e) SA stimulation of LNCaP-Enz-R cells also increased red fluorescence and decreased green fluorescence, further confirming the role of SA in improving mitochondrial function. (d, e) JC-1 fluorescence microscopy showing mitochondrial membrane potential changes. Scale bar = 50 μm. Data are expressed as the mean ± standard deviation of at least three independent experiments. Statistical significance was determined using one-way analysis of variance followed by Tukey's post hoc test ($^{*}p < 0.05$).

responses between hormone-sensitive and -resistant prostate cancer cells, the use of normal cells was beyond the mechanistic scope of this study. However, previous reports have indicated that SA exhibits minimal cytotoxicity in normal epithelial cells, supporting its selective anticancer potential. Second, although this study offers relevant insights into the molecular pathways underlying the anticancer properties of SA, further in vivo investigations are required to validate these results within a more biologically relevant setting. Third, the potential side effects and toxicity of SA were not assessed, which are critical for determining its therapeutic viability. Future studies should include a broader range of prostate cancer models, in vitro and in vivo, and investigate the long-term safety and efficacy of SA treatment to validate its potential as a therapeutic agent.

In summary, our study demonstrated that SA exerted its antimetastatic effects by activating mitochondrial biogenesis, enhancing $\Delta\Psi$m, and suppressing EMT. Therefore, SA emerges as a promising therapeutic agent for targeting metastasis in prostate cancer, particularly in cases resistant to conventional therapies such as enzalutamide. Another limitation is that no conventional chemotherapeutic drug was included as a positive control. Because the study aimed to elucidate the molecular mechanism of SA on AMPK-mediated EMT regulation rather than its cytotoxic potency, pathway-specific pharmacological modulators (AICAR and Compound C) were used instead of standard anticancer drugs. However, additional in vivo studies must be conducted to confirm these results and assess the potential clinical applications of SA in the treatment of metastatic prostate cancer. Future investigations should also explore the combination of SA with other therapeutic agents to evaluate its synergistic effects and optimize its therapeutic efficacy in overcoming treatment resistance.

5 | Conclusion

In conclusion, this study demonstrates that SA exerts significant anticancer effects in both hormone-sensitive LNCaP and enzalutamide-resistant LNCaP-Enz-R prostate cancer cells by simultaneously suppressing EMT and enhancing mitochondrial biogenesis. Mechanistically, SA activates the AMPK/PGC-1α/SIRT1/NRF1 signaling axis, leading to increased ATP production and stabilization of $\Delta\Psi$m. These mitochondrial improvements are closely associated with the upregulation of epithelial markers and the downregulation of key mesenchymal and EMT-associated transcription factors, thereby reducing cancer cell migration and metastatic potential. Importantly, the inhibitory effects of SA on EMT were attenuated by AMPK inhibition, confirming the central role of AMPK-mediated signaling in this process. Collectively, these findings identify SA as a promising mitochondrial-targeting agent capable of counteracting EMT and therapeutic resistance in prostate cancer, supporting its potential development as a complementary strategy for the treatment of advanced and CRPC.

Acknowledgments

We sincerely thank Dr. Szu-Chung Feng from the Department of Urology, Chang Gung Memorial Hospital, for generously providing the LNCap-Enz-R cell line used in this study. His support and contributions were invaluable to our research.

Funding

This study was supported by E-Da Hospital Research (grant nos. EDCHP112013 and NCKUEDA11310), and Kaohsiung Armed Forces General Hospital Research (grant no. KAFGH_D_109026).

Disclosure

The funders had no role in study design, data collection and analysis, decision to publish, or preparation of the manuscript.

Conflicts of Interest

The authors declare no conflicts of interest.

Data Availability Statement

The datasets generated and/or analyzed during the current study are available from the corresponding author on reasonable request.

References

1. E. M. Schaeffer, S. Srinivas, N. Adra, et al., "Prostate Cancer, Version 4.2023, NCCN Clinical Practice Guidelines in Oncology," *Journal of the National Comprehensive Cancer Network* 21, no. 10 (2023): 1067–1096, https://doi.org/10.6004/jnccn.2023.0050.

2. D. Ilic, M. Djulbegovic, J. H. Jung, et al., "Prostate Cancer Screening With Prostate-Specific Antigen (PSA) Test: A Systematic Review and Meta-Analysis," *BMJ* 362 (2018): k3519, https://doi.org/10.1136/bmj.k3519.

3. T. Chandrasekar, J. C. Yang, A. C. Gao, and C. P. Evans, "Mechanisms of Resistance in Castration-Resistant Prostate Cancer (CRPC)," *Translational Andrology and Urology* 4 (2015): 365–380.

4. J. P. Thiery, H. Acloque, R. Y. Huang, and M. A. Nieto, "Epithelial-Mesenchymal Transitions in Development and Disease," *Cell* 139, no. 5 (2009): 871–890, https://doi.org/10.1016/j.cell.2009.11.007.

5. C. Parker, E. Castro, K. Fizazi, et al., "Prostate Cancer: ESMO Clinical Practice Guidelines for Diagnosis, Treatment and Follow-Up," *Annals of Oncology* 31, no. 9 (2020): 1119–1134, https://doi.org/10.1016/j.annonc.2020.06.011.

6. T. M. Morgan, S. A. Boorjian, M. K. Buyyounouski, et al., "Salvage Therapy for Prostate Cancer: AUA/ASTRO/SUO Guideline Part II: Treatment Delivery for Non-Metastatic Biochemical Recurrence After Primary Radical Prostatectomy," *The Journal of Urology* 211, no. 4 (2024): 518–525, https://doi.org/10.1097/ju.0000000000003891.

7. S. C. Morgan, K. Hoffman, D. A. Loblaw, et al., "Hypofractionated Radiation Therapy for Localized Prostate Cancer: Executive Summary of an ASTRO, ASCO, and AUA Evidence-Based Guideline," *Pract Radiat Oncol* 8, no. 6 (2018): 354–360, https://doi.org/10.1016/j.prro.2018.08.002.

8. D. Ribatti, R. Tamma, and T. Annese, "Epithelial-Mesenchymal Transition in Cancer: A Historical Overview," *Translational Oncology* 13, no. 6 (2020): 100773, https://doi.org/10.1016/j.tranon.2020.100773.

9. P. A. Jing Yang, G. Berx, C. Blanpain, et al., "On Behalf of the EMT International Association (TEMTIA), Guidelines and Definitions for Research on Epithelial–Mesenchymal Transition," *Nature Reviews Molecular Cell Biology* 21 (2020): 341–352.

10. X. Li, C. Niu, G. Yi, et al., "Quercetin Inhibits the Epithelial-Mesenchymal Transition and Reverses CDK4/6 Inhibitor Resistance in Breast Cancer by Regulating circHIAT1/miR-19a-3p/CADM2 Axis," *PLoS One* 19, no. 7 (2024): e0305612, https://doi.org/10.1371/journal.pone.0305612.

11. M. L. Boland, A. H. Chourasia, and K. F. Macleod, "Mitochondrial Dysfunction in Cancer," *Frontiers Oncology* 3 (2013): 292, https://doi.org/10.3389/fonc.2013.00292.

12. Y. Liu, Y. Sun, Y. Guo, et al., "An Overview: The Diversified Role of Mitochondria in Cancer Metabolism," *International Journal of Biological Sciences* 19, no. 3 (2023): 897–915, https://doi.org/10.7150/ijbs.81609.

13. S. Pustylnikov, F. Costabile, S. Beghi, and A. Facciabene, "Targeting Mitochondria in Cancer: Current Concepts and Immunotherapy Approaches," *Translational Research* 202 (2018): 35–51, https://doi.org/10.1016/j.trsl.2018.07.013.

14. C. Canto, Z. Gerhart-Hines, J. N. Feige, et al., "AMPK Regulates Energy Expenditure by Modulating NAD+ Metabolism and SIRT1 Activity," *Nature* 458, no. 7241 (2009): 1056–1060, https://doi.org/10.1038/nature07813.

15. C. C. Chou, K. H. Lee, I. L. Lai, et al., "AMPK Reverses the Mesenchymal Phenotype of Cancer Cells by Targeting the Akt-MDM2-Foxo3a Signaling Axis," *Cancer Research* 74, no. 17 (2014): 4783–4795, https://doi.org/10.1158/0008-5472.can-14-0135.

16. D. G. Hardie, F. A. Ross, and S. A. Hawley, "AMPK: a Nutrient and Energy Sensor that Maintains Energy Homeostasis," *Nature Reviews Molecular Cell Biology* 13, no. 4 (2012): 251–262, https://doi.org/10.1038/nrm3311.

17. L. Z. Lingyan Wu, B. Li, H. Jiang, et al., "AMP-Activated Protein Kinase (AMPK) Regulates Energy Metabolism Through Modulating Thermogenesis in Adipose Tissue," *Frontiers in Physiology* 21, no. 9 (2018): 122, https://doi.org/10.3389/fphys.2018.00122.

18. T. L. Marin, B. Gongol, F. Zhang, et al., "AMPK Promotes Mitochondrial Biogenesis and Function by Phosphorylating the Epigenetic Factors DNMT1, RBBP7, and HAT1," *Science Signaling* 10, no. 464 (2017): eaaf7478, https://doi.org/10.1126/scisignal.aaf7478.

19. L. Wang and D. L. Brautigan, "alpha-SNAP Inhibits AMPK Signaling to Reduce Mitochondrial Biogenesis and Dephosphorylates Thr172 in AMPKalpha in Vitro," *Nature Communications* 4, no. 1 (2013): 1559, https://doi.org/10.1038/ncomms2565.

20. L. K. M. a.J. P. White, "The AMPK/p27Kip1 Pathway as a Novel Target to Promote Autophagy and Resilience in Aged Cells," *Cells* 10, no. 6 (2021): 1430.

21. M. Heidorn-Czarna, H. M. Heidorn, S. Fernando, et al., "Chronic Activation of AMPK Induces Mitochondrial Biogenesis Through Differential Phosphorylation and Abundance of Mitochondrial Proteins in *Dictyostelium discoideum*," *International Journal of Molecular Sciences* 22, no. 21 (2021): 11675, https://doi.org/10.3390/ijms222111675.

22. S. Herzig and R. J. Shaw, "AMPK: Guardian of Metabolism and Mitochondrial Homeostasis," *Nature Reviews Molecular Cell Biology* 19, no. 2 (2018): 121–135, https://doi.org/10.1038/nrm.2017.95.

23. G. He, G. Chen, W. Liu, et al., "Salvianolic Acid B: A Review of Pharmacological Effects, Safety, Combination Therapy, New Dosage Forms, and Novel Drug Delivery Routes," *Pharmaceutics* 15, no. 9 (2023): 2235, https://doi.org/10.3390/pharmaceutics15092235.

24. T. Qin, A. Rasul, A. Sarfraz, et al., "Salvianolic Acid A & B: Potential Cytotoxic Polyphenols in Battle Against Cancer via Targeting Multiple Signaling Pathways," *International Journal of Biological Sciences* 15, no. 10 (2019): 2256–2264, https://doi.org/10.7150/ijbs.37467.

25. J. Wang, Y. Ma, M. Guo, H. Yang, and X. Guan, "Salvianolic Acid B Suppresses EMT and Apoptosis to Lessen Drug Resistance Through AKT/mTOR in Gastric Cancer Cells," *Cytotechnology* 73, no. 1 (2021): 49–61, https://doi.org/10.1007/s10616-020-00441-4.

26. H. Zhang, J. Tang, Y. Cao, and T. Wang, "Salvianolic Acid B Suppresses Non-Small-Cell Lung Cancer Metastasis Through PKM2-Independent Metabolic Reprogramming," *Evidence-Based Complementary and Alternative Medicine* 2022 (2022): 9302403–9302413, https://doi.org/10.1155/2022/9302403.

27. Y. Zhang, W. Zhai, M. Fan, J. Wu, and C. Wang, "Salvianolic Acid B Significantly Suppresses the Migration of Melanoma Cells via Direct Interaction with beta-actin," *Molecules* 29, no. 4 (2024): 906, https://doi.org/10.3390/molecules29040906.

28. T. Mosmann, "Rapid Colorimetric Assay for Cellular Growth and Survival: Application to Proliferation and Cytotoxicity Assays," *Journal of Immunological Methods* 65, no. 1-2 (1983): 55–63, https://doi.org/10.1016/0022-1759(83)90303-4.

29. C. C. Liang, A. Y. Park, and J. L. Guan, "In Vitro Scratch Assay: A Convenient and Inexpensive Method for Analysis of Cell Migration in Vitro," *Nature Protocols* 2 (2007): 329–333, https://doi.org/10.1038/nprot.2007.30.

30. H. Towbin, T. Staehelin, and J. Gordon, "Electrophoretic Transfer of Proteins from Polyacrylamide Gels to Nitrocellulose Sheets: Procedure and Some Applications," *Proceedings of the National Academy of Sciences of the U S A* 76, no. 9 (1979): 4350–4354, https://doi.org/10.1073/pnas.76.9.4350.

31. S. T. Smiley, M. Reers, C. Mottola-Hartshorn, et al., "Intracellular Heterogeneity in Mitochondrial Membrane Potentials Revealed by a J-Aggregate-Forming Lipophilic Cation JC-1," *Proceedings of the National Academy of Sciences* 88, no. 9 (1991): 3671–3675, https://doi.org/10.1073/pnas.88.9.3671.

32. J. Li, B. Li, L. Luo, et al., "Increased Phenolic Acid and Tanshinone Production and Transcriptional Responses of Biosynthetic Genes in Hairy Root Cultures of Salvia przewalskii Maxim. Treated With Methyl Jasmonate and Salicylic Acid," *Molecular Biology Reports* 47, no. 11 (2020): 8565–8578, https://doi.org/10.1007/s11033-020-05899-1.

33. S.-C. H. Wei-Tang Chang, H.-L. Cheng, and S.-C. Chen, "Chin-Lin Hsu Rutin and Gallic Acid Regulates Mitochondrial Functions via the SIRT1 Pathway in C2C12 Myotubes," *Antioxidants* 10, no. 2 (2021): 286, https://doi.org/10.3390/antiox10020286.

34. V. Aggarwal, H. S. Tuli, A. Varol, et al., "Role of Reactive Oxygen Species in Cancer Progression: Molecular Mechanisms and Recent Advancements," *Biomolecules* 9, no. 11 (2019): 735, https://doi.org/10.3390/biom9110735.

35. H. Beltran, E. S. Antonarakis, M. J. Morris, and G. Attard, "Emerging Molecular Biomarkers in Advanced Prostate Cancer: Translation to the Clinic," *Am Soc Clin Oncol Educ Book* 35, no. 36 (2016): 131–141, https://doi.org/10.1200/edbk_159248.

36. E. B. Cristina Luceri, A. Pietro Femia, G. Caderni, L. Giovannelli, M. Lodovici, and M. Lodovici, "Aging Related Changes in Circulating Reactive Oxygen Species (ROS) and Protein Carbonyls are Indicative of Liver Oxidative Injury," *Toxicology Reports* 5 (2018): 141–145, https://doi.org/10.1016/j.toxrep.2017.12.017.

37. B. Congregado Ruiz, I. Rivero Belenchon, G. Lendinez Cano, and R. A. Medina Lopez, "Strategies to Re-Sensitize Castration-Resistant Prostate Cancer to Antiandrogen Therapy," *Biomedicines* 11, no. 4 (2023): 1105, https://doi.org/10.3390/biomedicines11041105.

38. H. M. Lin, B. Mak, N. Yeung, et al., "Overcoming Enzalutamide Resistance in Metastatic Prostate Cancer by Targeting Sphingosine Kinase," *EBioMedicine* 72 (2021): 103625, https://doi.org/10.1016/j.ebiom.2021.103625.

39. Y. T. Lin, Y. C. Huang, C. K. Liu, T. S. Lee, M. Chen, and Y. N. Chien, "Treatment-Emergent Co-Morbidities and Survival in Patients with Metastatic Castration-Resistant Prostate Cancer Receiving Abiraterone or Enzalutamide," *Frontiers in Pharmacology* 12 (2021): 669236, https://doi.org/10.3389/fphar.2021.669236.

40. E. L. B. D A Cottrell, G. M. Borthwick, M. A. Johnson, et al., "Role of Mitochondrial DNA Mutations in Disease and Aging," *Annals of the New York Academy of Sciences* 908 (2000): 199–207.

41. H. Liu, G. Li, B. Zhang, et al., "Suppression of the NF-kappaB Signaling Pathway in Colon Cancer Cells by the Natural Compound Riccardin D from Dumortierahirsute," *Molecular Medicine Reports* 17 (2018): 5837–5843.

42. K. S. Vikramdeo, A. Sharma, S. Anand, et al., "Mitochondrial Alterations in Prostate Cancer: Roles in Pathobiology and Racial Disparities," *International Journal of Molecular Sciences* 24, no. 5 (2023): 4482, https://doi.org/10.3390/ijms24054482.

43. Z. Wu, P. Puigserver, U. Andersson, et al., "Mechanisms Controlling Mitochondrial Biogenesis and Respiration Through the Thermogenic Coactivator PGC-1," *Cell* 98, no. 1 (1999): 115–124, https://doi.org/10.1016/s0092-8674(00)80611-x.